Frequency-dependent velocity smoothing in GPSPI migration

Chad M. Hogan and Gary F. Margrave

ABSTRACT

The GPSPI algorithm uses a phase shift that is a high-frequency approximation to the exact solution: the square-root Helmholtz operator symbol. The square-root Helmholtz operator symbol dramatically changes character between high- and low-frequency limits, while the GPSPI phase shift does not. A frequency-dependent smoothing of the velocity model (and therefore the phase shift) is used to approximate the character change of the square-root Helmholtz symbol, and is implemented via the spatial resampling within the FOCI algorithm. This results in heavy smoothing of the phase shift at low frequencies, and virtually no smoothing at higher frequencies. The frequency-dependent smoothing results in an image of much higher quality than the image generated using the usual GPSPI phase shift.

INTRODUCTION

The GPSPI algorithm (Margrave and Ferguson, 1999) provides a highly-accurate prestack depth migration algorithm. This algorithm depends upon a numerical implementation of the "infinitesimal extrapolator",

$$\begin{aligned}\Psi(x,z+\Delta z,\omega) &= \mathbf{T}_{\alpha(z:z+\Delta z)}\Psi(x,z,\omega)\\ &\approx \int_{\mathbb{R}} \phi(k_x,z,\omega)\alpha(x,k_x,\omega,z:z+\Delta z)e^{ik_x x}dk_x \end{aligned} \tag{1}$$

where

$$\alpha\left(x,k_x,\omega,z:z+\Delta z\right) = \begin{cases} \exp\left(i\Delta z\sqrt{\frac{\omega^2}{v(x)^2}-k_x^2}\right), & |k_x| \le \frac{|\omega|}{v(x)} \\ \exp\left(-\left|\Delta z\sqrt{\frac{\omega^2}{v(x)^2}-k_x^2}\right|\right), & |k_x| > \frac{|\omega|}{v(x)} \end{cases} . \tag{2}$$

Here Ψ represents the wavefield as a function of horizontal position x, vertical depth z, depth-step Δz, and temporal frequency ω. $\mathbf{T}$ is the infinitesimal extrapolation operator characterized by symbol α, where α is a function of x, horizontal wavenumber k_x, ω, and z. ϕ is the wavefield Ψ after Fourier-transforming from x to k_x. In this case, $\mathbf{T}$ extrapolates the wavefield from depth z to depth $z+\Delta z$. For a full description of this algorithm and its efficient implementation, see Margrave and Ferguson (1999) and Margrave et al. (2006).

THE SQUARE-ROOT HELMHOLTZ OPERATOR SYMBOL

Fishman (2002) identifies the term $\sqrt{\omega^2/v(x)^2-k_x^2}$ in equation 2 as the limiting form of a high-frequency approximation to the square-root Helmholtz operator symbol (i.e. an "infinite-frequency symbol"). Figure 1 shows the real part of the infinite-frequency symbol as used in GPSPI. This symbol is calculated for a velocity model consisting of three blocks of constant velocity. On the left, velocity v_1 is relatively high; in the middle, velocity v_2 is relatively low; and on the right, velocity v_3 is moderate. Figure 2 shows an ensemble of exact square-root Helmholtz operator symbols for high, moderate, low, and

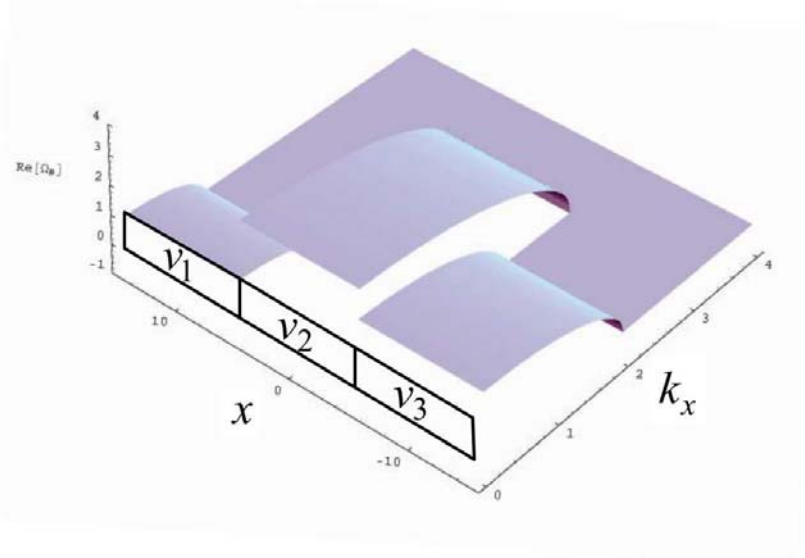

FIG. 1. Real part of the infinite-frequency square-root Helmholtz operator symbol for a velocity model with blocks of constant velocity. Adapted from Fishman (2002). This is the symbol as used in GPSPI.

zero frequency, also due to Fishman (2002). These symbols have been rotated to show the detail within the symbol. At high frequency, the symbol appears to be quite similar to the infinite-frequency symbol. The added ripple features capture the physics of the trapped horizontal modes – effectively the multiple horizontal reflections. The symbol at moderate frequency retains many of these features, but appears somewhat smoothed compared to the higher frequency symbol. The low-frequency symbol appears heavily smoothed, and the zero-frequency symbol shows only a single effective velocity. In an intuitive sense, these symbols are demonstrating that the various frequencies "see" different media. The highest frequencies are affected by all scales of structure within the velocity model, while the lowest frequencies see only the largest-scale overall velocity – any finite velocity changes are lost and only the background average velocity appears.

APPROXIMATING SYMBOLS

Although the symbol calculations given by Fishman (2002) are, at this point, far too computationally expensive for practical migration purposes, approximations may be considered. Specifically, we choose to preserve the apparent smoothing displayed by the symbols at various frequencies. Figure 3 again displays a three-block velocity model symbol at infinite frequency. Figure 4 shows this same symbol calculated with a velocity model that is smoothed with a smoothing length determined by the wavelength of low-frequency waves. The optimal method for smoothing remains an open problem, and at this point smoothing is done purely empirically.

TESTING

Testing of smoothed vs. unsmoothed symbols was performed using the FOCI (Margrave et al., 2006) method of GPSPI migration. The smoothing was accomplished using the spatial-resampling portion of the FOCI method. Although this spatial resampling was originally developed to address numerical stability and efficiency concerns, it effectively does

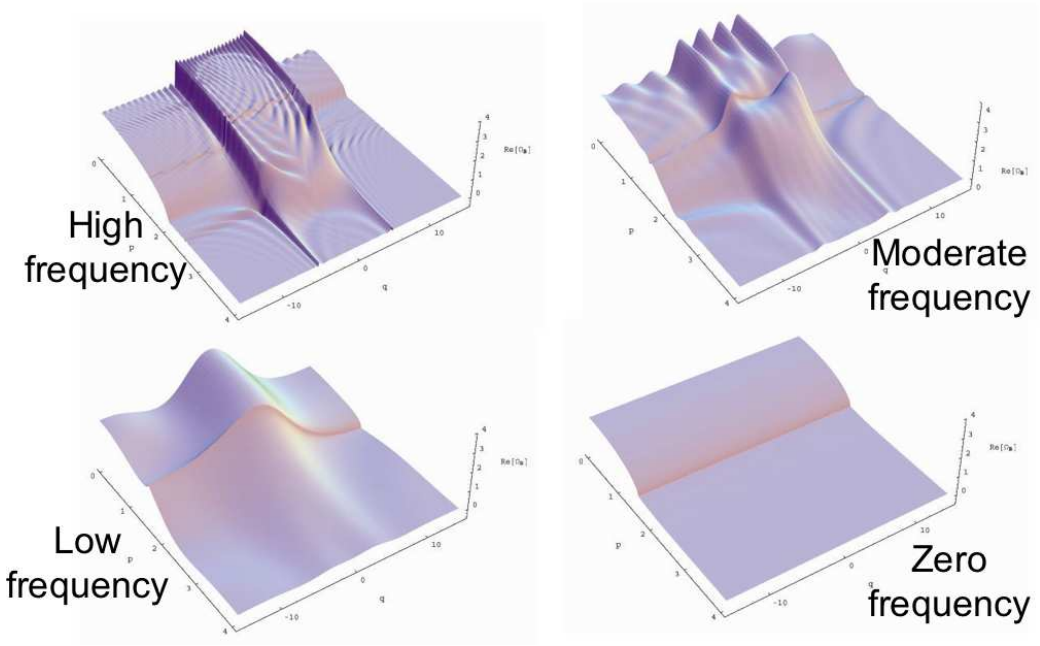

FIG. 2. Ensemble of real parts of the square-root Helmholtz operator symbols for a velocity model with blocks of constant velocity. Adapted from Fishman (2002).

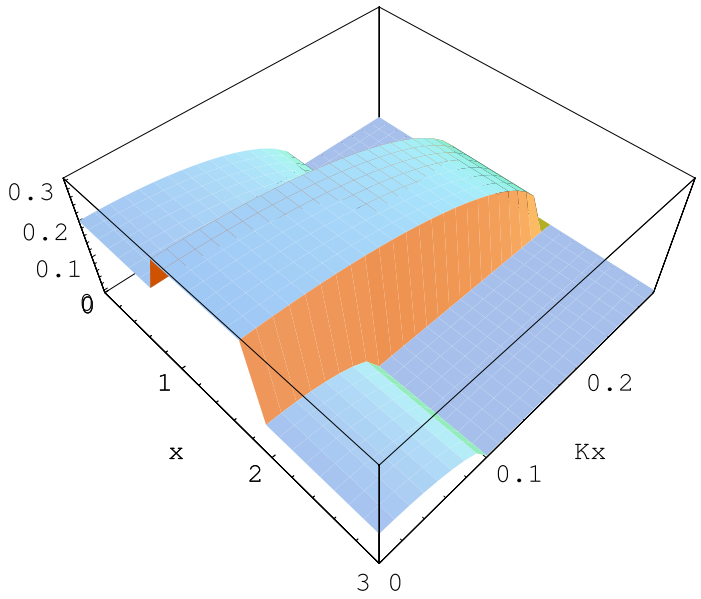

FIG. 3. Real part of the infinite-frequency symbol for the three-block velocity model.

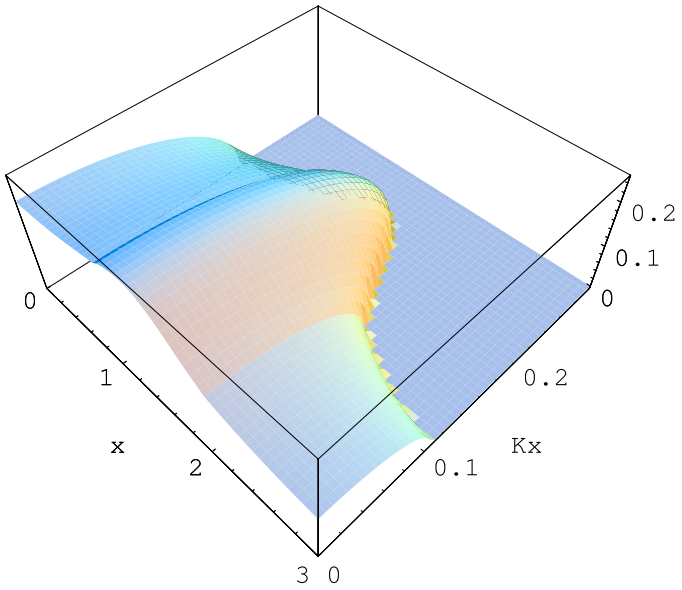

FIG. 4. Real part of the low-frequency symbol approximation (via smoothing of the velocity model) for the three-block velocity model.

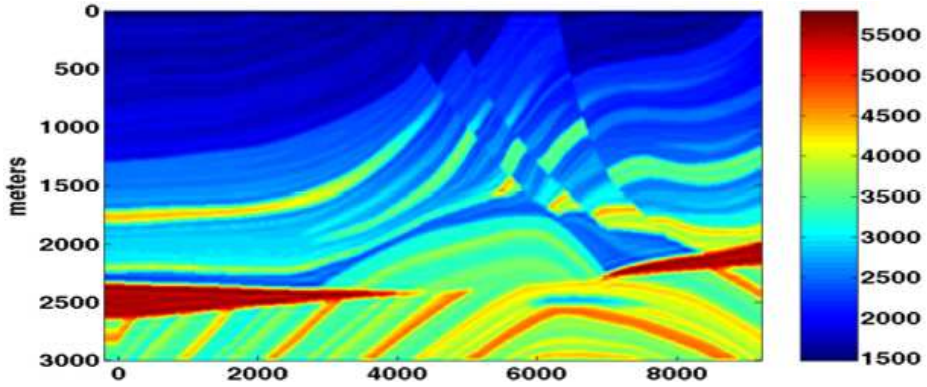

FIG. 5. The Marmousi velocity model. Velocities range between approximately $1500m/s$ and $5500m/s$.

perform a frequency-dependent smoothing of the velocity model. The smoothing method within spatial resampling is a simple spatial averaging. Migration tests were performed using synthetic data from the Marmousi model (Figure 5).

The FOCI spatial resampling typically decomposes the data into on the order of 10 frequency bands, ranging from low frequency ($\approx 4 - 6Hz$) to high frequency ($\approx 42 - 60Hz$). The velocity model is then smoothed with a spatial averaging that is characteristic for each frequency band.

Migrations were run both with and without spatial resampling. As the FOCI algorithm requires spatial resampling for stability and efficiency, special care was taken to ensure that these features were preserved in the unsmoothed case. Specifically, the image calculated using smoothed symbols had a final operator length of 31 points. In order to preserve stability and fidelity of the operator in the absence of the spatial resampling, the operator length had to be scaled in order to provide the same operator control within the wavelike region of propagation for each frequency band. Therefore, for the lowest frequency block, a

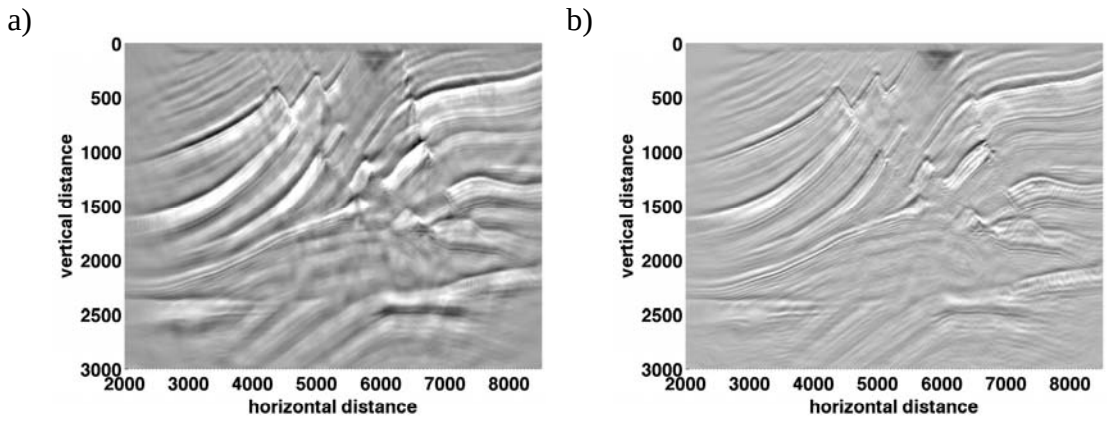

FIG. 6. Images of the Marmousi model generated a) without smoothing of the symbol and b) with smoothing of the symbol. The image generated with the smoothed symbol is clearly far superior to the image generated with the infinite-frequency symbol.

final operator length of more than 200 points was required. For a full description of spatial resampling and the division of the data into frequency bands, see Margrave et al. (2006).

The resulting images are shown in Figure 6. The image calculated with the smoothed symbol is clearly significantly better than the image calculated with the infinite-frequency symbol.

In order to determine the frequency-dependence of the difference in image quality, the concept of "residual" as defined by Hogan and Margrave (2006) was used. The smoothed- and unsmoothed-symbol images were broken into frequency bands 10 Hz wide, centred every 5 Hz from 5 to 55 Hz. 11 new images were generated, each image consisting of the unsmoothed-symbol image with one frequency band replaced by the respective frequency band from the smoothed-symbol image. For example, the first image was generated with the 5-15 Hz band from the smoothed-symbol image, along with all other 10 bands from the unsmoothed-symbol image. Each of these images was compared with an image composed of all 11 bands of the unsmoothed-symbol image. The residuals are plotted in Figure 7.

These residuals indicate that the smoothing of the symbol had the most effect on the image in the lower frequencies, and had very little effect on higher frequencies. This matches our expectations that the biggest differences in the symbol will be found in the lower frequency bands and so the biggest improvement in overall quality will be found there as well.

CONCLUSIONS AND FUTURE WORK

The frequency dependence found in the exact square-root Helmholtz operator symbol is striking and leads to symbols that are dramatically different from the infinite-frequency symbols that are used in standard GPSPI migration. Although these exact operator symbols are extremely difficult to compute, a qualitative and possibly naïve approximation to these symbols based on frequency-dependent smoothing of the underlying velocity model results in an image that is far superior to one that is calculated with just the infinite-frequency symbol.

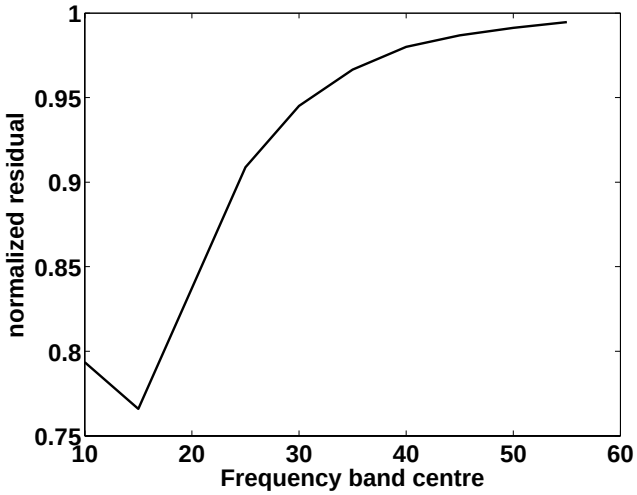

FIG. 7. Determination of effectiveness of symbol smoothing as a function of frequency. Lower residuals indicate that the smoothing of the symbol resulted in a change in quality of the overall image, while a residual of 1 indicates that the smoothing had little to no effect in this region.

The FOCI algorithm may already be implemented with a simple but effective form of symbol smoothing: spatial resampling following Margrave et al. (2006). Therefore, in addition to providing greater computational efficiency and numerical stability to the imaging, this spatial resampling also adds somewhat more accurate physics to the wavefield extrapolation and therefore a better image.

We are currently working to understand how to optimally approximate the exact square-root Helmholtz symbol in order to maximize the image quality.

REFERENCES

Fishman, L., 2002, Applications of directional wavefield decomposition, phase space, and path integral methods to seismic wave propagation and inversion: Pure and Applied Geophysics, **159**, 1637–1679.

Hogan, C. M., and Margrave, G. F., 2006, Measurement of convergence in plane-wave migration, Tech. rep., CREWES Research Report.

Margrave, G. F., and Ferguson, R. J., 1999, Wavefield extrapolation by nonstationary phase shift: Geophysics, **64**, 1067–1078.

Margrave, G. F., Geiger, H. D., Al-Saleh, S. M., and Lamoureux, M. P., 2006, Improving explicit depth migration with a stabilizing Wiener filter and spatial resampling: Geophysics, **71**, S111–S120.